Numerical multi-scale simulations of the mechanical behavior of β-metastable titanium alloysTi5553 andTi 17

Guillaume Martin, Loic Nazé, Georges Cailletaud

ELSEVIER

Numerical multi-scale simulations of the mechanical behavior of β-metastable titanium alloys Ti5553 and Ti17

G. Martin[a,b], L. Nazé[a], G. Cailletaud[a]

[a]*Centre des Matériaux, ENSMP ParisTech, UMR CNRS 7633, BP87, 91003 Évry, France*
[b]*Snecma Villaroche, Rond-point René Ravaud - Réau 77550 Moissy-Cramayel*

Abstract

The purpose of this study is to investigate the deformation mechanisms in the β-metastable titanium alloys Ti17 and Ti5553, which exhibit an important fraction of β phase (∼40%). A mean field model is introduced to depict the effect of microstructure on mechanical properties. The average behavior of each phase is taken into account: the micromechanical model simulates for each phase the respective elastic anisotropy and the visco-plastic flow with kinematic and isotropic hardening. A good agreement has been obtained between numerical simulations and experiments for several microstructures.
©2011 Published by Elsevier Ltd. Selection and/or peer-review under responsibility of ICM11

Keywords: β-metastable titanium alloys, time dependent crystal plasticity, mean field model
PACS: 4635.+z   *2010 MSC:* 74A60 74C10 74D10 74M25 74Q05

1. Introduction

Two β-metastable titanium alloys are considered in this study: Ti-5553 and Ti-17. Even though β-metastable titanium alloys have been used for more than 30 years, few studies have been carried out and uncleared questions remain, particularly the role of the β phase (∼40%) in the deformation process. Within this context, different numerical models are developed to simulate the deformation mechanisms of Ti5553 and Ti17 at various scales. They are calibrated by means of a large data base of mechanical tests under monotonic loading [pc 1-2][1].
Especially, a mean field mesoscopic model is proposed, involving specific constitutive equations adapted to each phase. The β phase (BCC), exhibiting many slip systems, is rendered by a von Mises criterion, whereas crystal plasticity is used for the α (HCP) phase variants. The selected families of slip systems the in α phase are basal $\langle \underline{a} \rangle$, prismatic $\langle \underline{a} \rangle$, pyramidal $\pi_1 \langle \underline{a} \rangle$ and pyramidal $\pi_1 \langle \underline{c} + \underline{a} \rangle$.

Both materials are presented in the first part of the paper. In a second part, the multi-phase elasto-visco-plastic model is described. Comparisons between simulations and experiments are shown in the last section.

2. Microstructures and properties of β-metastable titanium alloys

The so-called "β-metastable" titanium alloys are those which retain a large volume fraction ($\sim 40\%$) of β phase at room temperature after heat treatment. The microstructure is composed of former β-grains, the α phase precipitating within with various morphologies: needles, nodules, ... (Fig. 1).
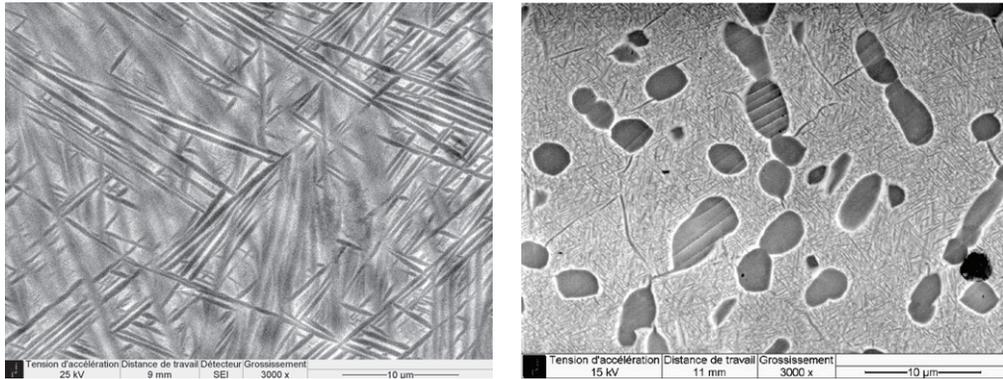

Figure 1: Microstructures of Ti17 (left) and Ti5553 (right) from SEM [pc 2]: β phase is white and α phase is dark.

For each former β-grain, twelve different crystal orientations of the α precipitates (variants) are available according to the Burgers relationship [1], which links particular crystal directions and planes of both phases:

$$< 111 >_\beta \ // \ < 11\bar{2}0 >_\alpha \ , (110)_\beta // (0001)_\alpha$$

Consequently, the computation is performed at three different levels: macroscopic, grain and variant scales. The transition between the three bases is achieved by two rotation matrices:

- The first one rules the transition from the macroscopic specimen basis to the β-grain basis. The rotation matrix is determined from the grain orientation measurements by EBSD in SEM [pc 2];

- The second one corresponds to the transition from the β-grain basis to one of the twelve α variants bases which belong to the same grain.

In the model which will be presented next, the α variants are considered as elliptic cylindrical inclusions: thus, the associate Eshelby tensor, $\mathbf{S}_\alpha$, will be written as in [2]. However, the β matrix will be considered as a spherical inclusion, which leads to an Eshelby tensor $\mathbf{S}_\beta$ as expressed in [3].

Furthermore, the elastic behavior of both phases will be linked to their crystallographic structures: the stiffness tensor of α variants will have a transversely isotropic symmetry because of its hexagonal structure, whereas the stiffness tensor of the β phase will exhibit a cubic symmetry, due to its BCC structure.

3. Model description

In his self-consistent approach for elasto-plasticity behavior in polycrystals, Hill[4] introduced the local behavior of each phase *i* through a linearly incremental formulation:

$$\dot{\sigma}_i = \underset{\sim}{\mathbf{L}}_i : \dot{\varepsilon}_i \tag{1}$$

At the macroscopic scale, the constitutive equation given by Hooke's law for the elastic case is extended to the elastic-plastic regime. The tangent stiffness $\underset{\sim}{\mathbf{L}}^{eff}$ is a fourth-rank operator that relates stress and strain rates:

$$\dot{\underset{\sim}{\Sigma}} = \underset{\sim}{\mathbf{L}}^{eff} : \dot{\mathbf{E}} \tag{2}$$

The stress rate within each phase is uniform and can be expressed as:

$$\dot{\sigma}_i = \dot{\underset{\sim}{\Sigma}} + \underset{\sim}{\mathbf{L}}_i^{\star} : (\dot{\mathbf{E}} - \dot{\varepsilon}_i) \tag{3}$$

where $\underset{\sim}{\mathbf{L}}^{\star}$ is the tangent operator for the phase. It can further be shown that this fourth-rank tensor depends on $\underset{\sim}{\mathbf{L}}^{eff}$ and on Eshelby tensor $\underset{\sim}{\mathbf{S}}_i$, which introduced a phase morphology dependence. One thus has:

$$\underset{\sim}{\mathbf{L}}_i^{\star} = \underset{\sim}{\mathbf{L}}^{eff} : (\underset{\sim}{\mathbf{S}}_i^{-1} - \underset{\sim}{\mathbf{I}}) \tag{4}$$

Combining the global (2) and local (1) constitutive equations in the previous expression (4) yields to a direct relation between local stress rate and global strain rate:

$$\dot{\sigma}_i = \underset{\sim}{\mathbf{L}}_i : (\underset{\sim}{\mathbf{L}}_i + \underset{\sim}{\mathbf{L}}_i^{\star})^{-1} : (\underset{\sim}{\mathbf{L}}^{eff} + \underset{\sim}{\mathbf{L}}_i^{\star}) : \dot{\mathbf{E}} \tag{5}$$

Knowing that the weighted average of the stress of all phases is equal to that of the bulk material: $\dot{\underset{\sim}{\Sigma}} = \langle \dot{\sigma}_i \rangle$, an implicit expression of $\underset{\sim}{\mathbf{L}}^{eff}$ is obtained:

$$\underset{\sim}{\mathbf{L}}^{eff} = \left\langle \underset{\sim}{\mathbf{L}}_i : \left[\underset{\sim}{\mathbf{L}}_i + \underset{\sim}{\mathbf{L}}^{eff} : (\underset{\sim}{\mathbf{S}}_i^{-1} - \underset{\sim}{\mathbf{I}}) \right]^{-1} : \left[\underset{\sim}{\mathbf{L}}^{eff} : \underset{\sim}{\mathbf{S}}_i^{-1} \right] \right\rangle \tag{6}$$

The differential equations are integrated by means of an explicit algorithm using Runge-Kutha (RK2) method. For the sake of simplicity, the tangent operator is constant during a time increment, and its value is estimated from the previous increment. It is worth noting that the present formulation is a mixture of Hill's self-consistent formulae and of a time dependent local mode, so that its self-consistent character is not fully preserved. It is assumed that both global and local responses remain relevant, due to the low rate dependency in the constitutive equations.

$$\underset{\sim}{\mathbf{L}}_{[t]}^{eff} = \left\langle \underset{\sim}{\mathbf{L}}_i : \left[\underset{\sim}{\mathbf{L}}_i + \underset{\sim}{\mathbf{L}}_{[t-\Delta t]}^{eff} : (\underset{\sim}{\mathbf{S}}_i^{-1} - \underset{\sim}{\mathbf{I}}) \right]^{-1} : \left[\underset{\sim}{\mathbf{L}}_{[t-\Delta t]}^{eff} : \underset{\sim}{\mathbf{S}}_i^{-1} \right] \right\rangle \tag{7}$$

The computation of the instantaneous stiffness of each phase is done iteratively, using the incremental expressions of the stress and strain rates:

$$\underset{\sim}{\mathbf{L}}_i = \frac{\Delta \sigma_i}{\Delta \varepsilon_i} \tag{8}$$

To determine this relation, the strain rate in the phase *i* is decomposed into an elastic part and a visco-plastic part. For both phases, phenomenological models with hardening variables are used

to described the plastic strain evolution. For the von Mises formulation, the loading function f is related to the von Mises stress invariant J:

$$f(\underset{\sim}{\sigma}_i, \mathbf{X}, R) = J(\underset{\sim}{\sigma}_i - \underset{\sim}{\mathbf{X}}) - R \qquad \text{with } J(\underset{\sim}{\sigma}_i - \underset{\sim}{\mathbf{X}}) = \sqrt{\frac{3}{2}(\mathbf{s}_i : \mathbf{s}_i)} \qquad (9)$$

where $\underset{\sim}{\mathbf{X}}$ is the back stress of kinematic hardening, R is the isotropic hardening and $\mathbf{s}_i$ is the deviatoric part of $\underset{\sim}{\sigma}_i - \underset{\sim}{\mathbf{X}}$. This loading function is then used to define the cumulated strain and the hardening parameters evolution:

$$\dot{p} = \left\langle \frac{f}{K} \right\rangle^n \qquad \text{with } \langle x \rangle = \max(x, 0) \qquad (10)$$

$$\mathbf{X} = \frac{2}{3}C\underset{\sim}{\alpha} \qquad \text{with } \dot{\underset{\sim}{\alpha}} = \left(\underset{\sim}{\mathbf{n}} - D\underset{\sim}{\alpha} \right)\dot{p} \qquad (11)$$

$$R = R_0 + bQr \qquad \text{with } \dot{r} = (1 - br)\dot{p} \qquad (12)$$

C and D are material parameters, R_0 is the plastic threshold, Q is the hardening capacity and b is the parameter defining saturation rate. So, total strain rate will be:

$$\dot{\underset{\sim}{\varepsilon}}_i = \dot{\underset{\sim}{\varepsilon}}^{\mathbf{e}}_i + \dot{\underset{\sim}{\varepsilon}}^{\mathbf{p}}_i = \underset{\sim}{\mathbf{C}}^{-1}_i : \dot{\underset{\sim}{\sigma}}_i + \dot{p}\,\underset{\sim}{\mathbf{n}} \qquad (13)$$

For crystal plasticity[5], each system s has its own criterion:

$$f^s(\tau^s, x^s, r^s) = | \tau^s - x^s | - r^s \qquad (14)$$

and:

$$\dot{\upsilon}^s = \left\langle \frac{f^s}{K} \right\rangle^n \qquad \text{with } \langle x \rangle = \max(x, 0) \qquad (15)$$

$$x^s = \frac{2}{3}C\alpha^s \qquad \text{with } \dot{\alpha}^s = (sign(\tau^s - x^s) - D\alpha^s)\dot{\upsilon}^s \qquad (16)$$

$$r^s = \tau_c^s + Q \sum_r h_{sr} b \rho^r \qquad \text{with } \dot{\rho}^r = (1 - b\rho^r)\dot{\upsilon}^r \qquad (17)$$

where $\dot{\upsilon}^s$ is the cumulated shear strain rate in one slip system s, τ_c^s is the critical resolved shear stress beyond which the slip system s is activated, h_{sr} represents the interaction matrix between slip systems, and $\mathbf{m}^s$ is the Schmid tensor, which relies the local shear stress in one slip system to the stress tensor: $\tau^s = \underset{\sim}{\sigma}_i^s : \underset{\sim}{\mathbf{m}}^s$. This leads to:

$$\dot{\underset{\sim}{\varepsilon}}_i = \dot{\underset{\sim}{\varepsilon}}^{\mathbf{e}}_i + \dot{\underset{\sim}{\varepsilon}}^{\mathbf{p}}_i = \underset{\sim}{\mathbf{C}}^{-1}_i : \dot{\underset{\sim}{\sigma}}_i + \sum_s \dot{\upsilon}^s sign(\tau^s - x^s)\underset{\sim}{\mathbf{m}}^s \qquad (18)$$

To reach the expression of $\underset{\sim}{\mathbf{L}}_i$ in both cases, we derive from $\dot{\underset{\sim}{\sigma}}$ these expressions and we take their incremental form. The inversion give us the sought equations. First, for the von Mises approach:

$$\underset{\sim}{\mathbf{L}}_i = \left[\frac{\Delta \underset{\sim}{\varepsilon}_i}{\Delta \underset{\sim}{\sigma}_i} \right]^{-1} = \left[\underset{\sim}{\mathbf{C}}^{-1}_i + \frac{n}{K}\left(\frac{J(\underset{\sim}{\sigma}_i - \mathbf{X}) - R}{K} \right)^{n-1} \Delta t\, \mathbf{n} \otimes \underset{\sim}{\mathbf{n}} + \left(\frac{J(\underset{\sim}{\sigma}_i - \mathbf{X}) - R}{K} \right)^n \Delta t\, \underset{\sim}{\mathbf{N}} \right]^{-1} \qquad (19)$$

where $\underset{\sim}{\mathbf{N}}$ is a fourth-rank tensor which depends on the Jacobian tensor $\underset{\sim}{\mathbf{J}}$ which is the link between a second-rank tensor and its deviator: $\mathbf{s}_i = \underset{\sim}{\mathbf{J}} : \underset{\sim}{\sigma}_i$. Then, $\underset{\sim}{\mathbf{N}}$ can be written as:

$$\underset{\sim}{\mathbf{N}} = \frac{1}{J(\sigma_i)} \left(\frac{3}{2} \mathbf{s}_i \otimes \underset{\sim}{\sigma}_i^{-1} - \underset{\sim}{\mathbf{n}} \otimes \underset{\sim}{\mathbf{n}} \right) \tag{20}$$

And for crystal plasticity:

$$\underset{\sim}{\mathbf{L}}_i = \left[\underset{\sim}{\mathbf{C}}_i^{-1} + \sum_s \frac{n}{K} \left(\frac{|\tau^s - x^s| - r^s}{K} \right)^{n-1} \Delta t \; sign(\tau^s - x^s) \; \underset{\sim}{\mathbf{m}}^s \otimes \underset{\sim}{\mathbf{m}}^s \right]^{-1} \tag{21}$$

Once plastic flow rate has been computed, using visco-plastic flow rules presented above, the elastic part of the deformation can be deduced from the local plastic strain rate and equation (3):

$$\dot{\underset{\sim}{\varepsilon}}^{\mathbf{e}}_i = (\underset{\sim}{\mathbf{C}}_i + \underset{\sim}{\mathbf{L}}_i^{\star})^{-1} : (\underset{\sim}{\mathbf{L}}^{eff} : \underset{\sim}{\mathbf{S}}^{-1} : \dot{\underset{\sim}{\mathbf{E}}} - \underset{\sim}{\mathbf{L}}_i^{\star} : \dot{\underset{\sim}{\varepsilon}}^{\mathbf{p}}_i) \tag{22}$$

This will allow us to evaluate the stress in the next step.

4. Results

This model has been implemented as a user material of the ZSet/Zébulon[6]. Some simulations are carried out with 25 β-grains and compared with experimental uniaxial tensile tests [pc 1-2] (Fig.2). Ti17 was supplied by Snecma, whereas Ti5553 was provided by Messier-Dowty. For each titanium alloy, three different microstructures have been studied: a 100% β polycrystal and two two-phase microstructures with various fractions of α phase. The first one exhibits coarse α precipitates and a medium α phase volume fraction, while the second one shows a finer precipitation of α phase and a higher α phase volume fraction. Specimens diameter is 6 mm and applied strain rate is maintained between $10^{-3} s^{-1}$ and $2.10^{-3} s^{-1}$.
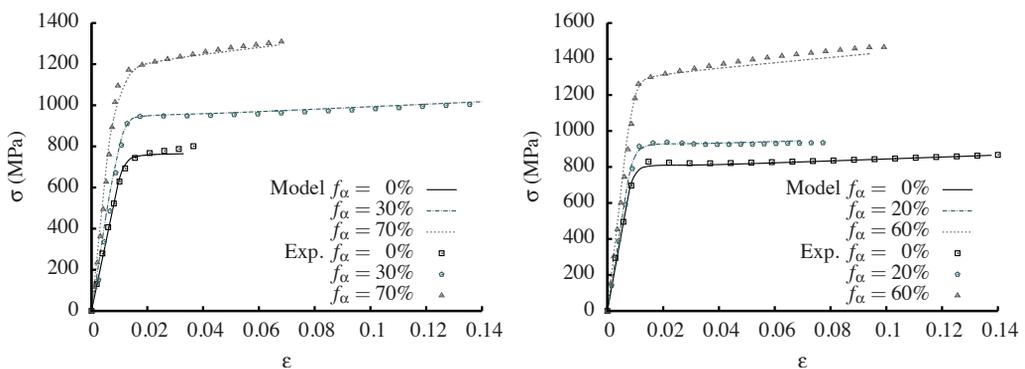

Figure 2: Macroscopic uniaxial tensile tests [pc 1-2] and fitted model predictions for Ti17 microstructures (left) and Ti5553 ones (right)

Fig.2 shows the macroscopic stress-strain curves for each titanium alloy. The material parameters for the β phase were first identified thanks to the 100% β microstructure. Then, the

parameters belonging to the α phase were deduced using the tensile curves of the two-phase microstructures.

In these simulations, the yield stress R_0 of the β phase and the critical resolved shear stress of the slip systems τ_c^s in α phase change with the microstructure. This can be justified by the fact that the increase of α phase volume fraction leads to a higher confinement of dislocations in both phases, which increases as well the plastic flow resistance. Moreover, the hardening slope, which is ruled by kinematic hardening, raises with the size of α precipitates because of the increase of α/β interfaces, which are obstacles to dislocations motion.

It appears that the model predictions are in good agreement with experiment: the specific elastic moduli has been correctly evaluated in function of the respective volume fractions of each phase and the plastic flow is well predicted.

5. Concluding remarks and perspectives

A specific multi-phase elasto-visco-plastic model has been developed to predict the mechanical behavior of two titanium alloys, accounting to the respective phase fractions and properties.

Comparisons with experiment have proved that the model is effective at predicting the behavior of Ti5553 and Ti17 and, consequently, it will be used in forthcoming frameworks, such as the simulation of the global and local behavior of a large grain 200 μm thick specimen tested at the PPRIME laboratory [pc 2].

An explicit representation of the microstructure will be then required: for each β-grains, we will attribute a real geometry and crystallographic orientation. Both phases will be represented at the grain level, by means of the model presented in this article. The comparison between experiment and simulation will be made on global tension curves as well as on a meso-level, by considering full field measurements of the out-of-plane displacement and of the strain field.

Acknowledgements

References

[1] W. Burgers, On the process of transition of the cubic-body-centered modification into the hexagonal-close-packed modification of zirconium, Physica 1 (1934) 561–586.
[2] B. Kim, H. Lee, Closed form solution of the exterior-point Eshelby tensor for an elliptic cylindrical inclusion, J. of Applied Mechanics 77.
[3] T. Mura, Micromechanics of defects in solids, Martinus Nijhoff, 1987.
[4] R. Hill, Continuum micro–mechanisms of elastoplastic polycrystals, J. Mech. Phys. Sol. 13 (1965) 89–101.
[5] G. Cailletaud, A micromechanical approach to inelastic behaviour of metals, Int. J. of Plasticity 8 (1992) 55–73.
[6] Transvalor, ENSMP, ZéBuLon 8.4.4 References Manuals, Northwest Numerics, 2010.